Peer-reviewed version available at *Energies* **2019**, *12*, 167; doi:10.3390/en12010167

An Ant Colony Optimized MPPT with Single Cuk Converter for Standalone Hybrid PV-Wind Power Generation for Residential Applications and Changing Operating Conditions

Neeraj Priyadarshi[1,*], Vigna K. Ramachandaramurthy[2], Sanjeevikumar P [3,*], FarooqueAzam[1]

[1] Department of Electrical Engineering, Millia Institute of Technology, Purnea-854301, India; neerajrjd@gmail.com (N.P.);farooque53786@gmail.com (F.A.)
[2] Institute of Power Engineering, Department of Electrical Power Engineering, Universiti Tenaga Nasional, Kajang 43000, Malaysia; vigna@uniten.edu.my (V.K.R.)
[3] Department of Energy Technology, Aalborg University, 6700 Esbjerg, Denmark
* Correspondence: neerajrjd@gmail.com (N.P.)

Abstract-This research work explains the practical realization of hybrid solar wind based standalone power system with maximum power point tracker (MPPT) to produce electrical power in rural places (residential applications). The solar inspired Ant Colony Optimization (ACO) based MPPT algorithm is employed for the purpose of fast and accurate tracking power from solar and wind system. Fuzzy Logic Control (FLC) inverter controlling strategy is adopted in this presented work compared to classical PI control. Moreover, single Cuk converter is operated as impedance power adapter to execute MPPT functioning. Satisfactory practical results have been realized using dSPACE (DS1104) platform that justify the superiority of proposed algorithms designed under various operating situations.

Keywords: Ant Colony Optimization; Cuk converter; dSPACE (DS1104); Fuzzy Logic Control

1.INTRODUCTION

Because of abounded necessity of energy harvest and continuous depletion of fossil fuels, demands of renewable energy sources are gaining more attention. Photovoltaic (PV) and wind are the environment friendly renewable energy sources, which has more contemplation for backwoods utilization. Standalone wind energy conversion system (WECS) / PV system have been remarkably employed to produce electrical power in rural places for agricultural applications [1-3]. Nevertheless, fluctuations in solar insolation level and wind speed are the major shortcomings of these renewable sources. Compared to individual PV/wind system, the hybrid PV/wind integrated system provides high steady power generation. However, implementation of hybrid PV/wind systems is being future assignments for researchers. It is also noted that in contrast to individual PV/wind system, the hybrid system has low cost of implementation with augmented steady operation.

Particularly, Permanent Magnet Synchronous Generator (PMSG) is enlisted prevalence for variable speed WECS and has lossless rotor with limited stator winding and core power losses. WECS coupled PMSG provides power generation under low speed region with gearless mechanism which has high efficiency and reliability compared to gearbox system [4-5].Maximum Power point tracking (MPPT) methods are essential constituent for fast exact tracking of global maxima and competency to achieve peak power generation under non-uniform environmental conditions. A detailed literature look has been provided viz. perturb and observe (P&O); Hill climbing (HC) and incremental conductance (INC) [6-8]. Nevertheless, mentioned algorithms lose control under non-uniform weather conditions. Intelligent MPPT algorithms such as Fuzzy Logic Control (FLC), Artificial Neural Network (ANN) methods have been exercised for peak power extraction under abrupt operating conditions [9-10]. However, by virtue of ample neurons, tracking data requirement and complex fuzzy inference indicated algorithms

are not applicable for lesser expense microcontroller. However, soft computing occupied MPPT algorithms are preferred for exact exploration of maximum power point (MPP). Several soft computing algorithms such as particle swarm optimization (PSO), evolutionary algorithm Viz. firefly algorithm (FA), artificial bee colony (ABC), Flower pollination (FP); Grey wolf optimization methods have been reported in literature survey [11-15].

PSO technique consists of large number of iterations which results diversion from MPP with slow updating speed. Belhachat et.al [16] has combined the performance of various MPPT techniques, which reveals that ANT Colony Optimization (ACO) method has relatively simpler implementation, very fast tracking velocity and high efficiency compared to other algorithms discussed in literature. Sundeswaran et al. [17] has implemented cascaded P & O assisted ANT Colony Optimization (ACO) method for rapid PV power tracking using PIC16F876A microcontroller.Under partial shading situations, the behavior has been examined which provides fast global searching and convergence. However, authors have discussed proposed MPPT algorithm for particular PV system power generation. Emerson et al. [18] presented ACO algorithm for PV-fuel cell integration with islanding employed with boost converter. However, there is no experimental work carried out for the system verification and analysis of power quality issues. In this paper, an ANT Colony Optimization based MPPT technique has been employed to get acceptable solutions in non-linear operating conditions compared to other method discussed in literature. The ACO based MPPT provides rapid battery changing operation with lesser dispersion of battery for hybrid PV-wind power system.

Several DC-DC converters have been reviewed for MPPT purpose, which is responsible for load matching and converts peak powers from renewable sources to load. Generally, buck, boost, buck-boost, SEPIC, Zeta, Cuk converters are considered dc-dc converters for MPPT operation which accomplish impedance balance between renewable sources and load [19-20]. Buck boost converters are unable to handle MPPT operations under changing weather conditions. Moreover, compared to SEPIC and Cuk converters, buck ,boost, buck-boost and Zeta converter require high cost driver circuits with supplementary blocked diode for preventing reversal current from battery. Equated with presented dc-dc converter topologies, Cuk converter is adequate to provide MPPT operation through entire PV/wind characteristics under every changing operating conditions with less input current ripple and inverted output.Particular power converters with battery back up have been used for hybrid PV-wind power generation systems implementations. Furthermore, individual powers converters are regulated with multiplex methods for optimal power generation which consequence conduction and switched loss in power converters.

In this research work, a single Cuk converter is employed for improvement of power conversion efficiency by reducing the power level translation. Moreover, in this hybrid PV-wind system, a Cuk converter is straightly coupled with DC link voltage rather than using dc-dc converter. The Cuk converter is placed between PMSG coupled rectifier and inverter, which is responsible DC, link voltage regulations. The Cuk converters output acts as a load line to the solar module. With the application of FLC current controller, the inverter current can be regulated using PV-wind systems [21]. However, in traditional topology the dc-dc converter is employed after PV module for optimal tracking of power.

Included work, based on ACO MPPT has no requirement of supplement circuitry with voltage/current sensors and independent system responses compared to different evolutionary techniques used. Novelty of this research paper is MPPT action with ACO technique followed by FLC inverter controller for residential PV-Wind power generation has neither been discussed nor implemented experimentally under changing operating conditions with single Cuk converter as an impedance balancer using dSPACE (DS1104) platform.

Preprints (www.preprints.org) | NOT PEER-REVIEWED | Posted: 3 September 2018 doi:10.20944/preprints201809.0031.v1

Peer-reviewed version available at Energies 2019, 12, 167; doi:10.3390/en12010167

2.Complete Schematic of PV-Wind System

Fig. 1 demonstrates standalone hybrid PV-wind- Battery power system comprises of PV modules, PMSG based WECS, battery, voltage source inverter (VSI) and load. The ACO based MPPT is employed with single Cuk converter is operating in hybrid power generation for residential application. FLC-dSPACE based controller is used for inverter voltage regulation to retain inverter voltage regulation and frequency invariable. The employed Cuk converter imparts consistent DC link voltage for charging of battery by application of ACO MPPT.

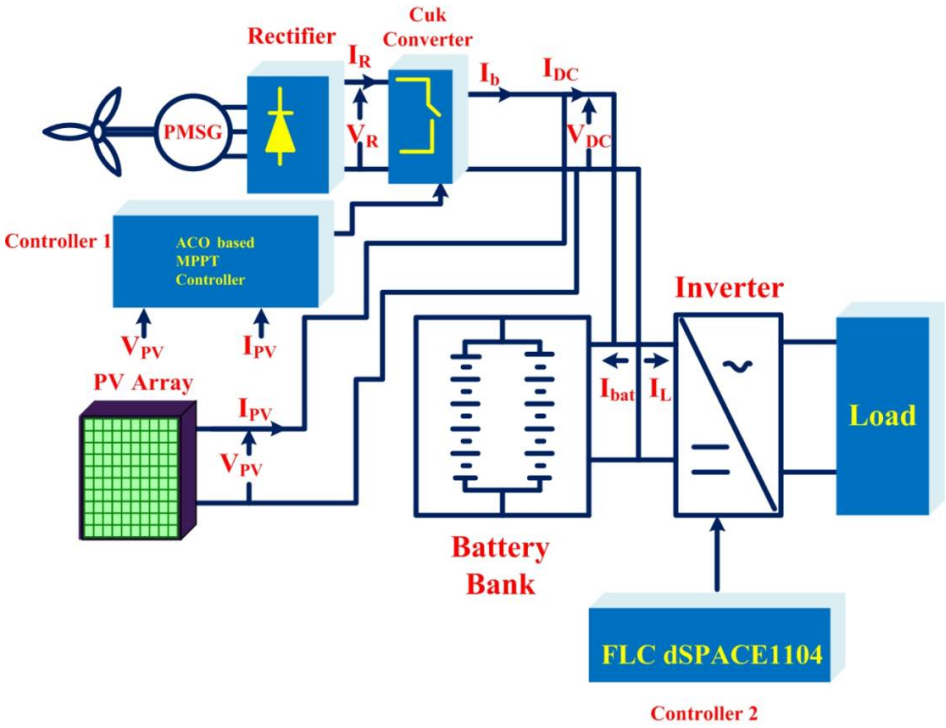

(a)

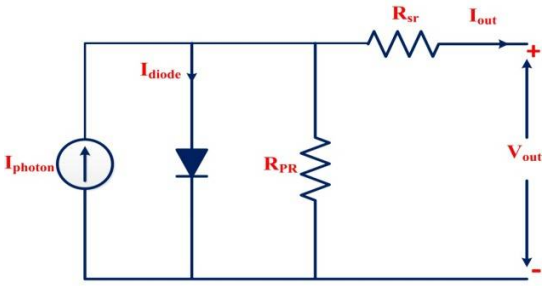

(b)

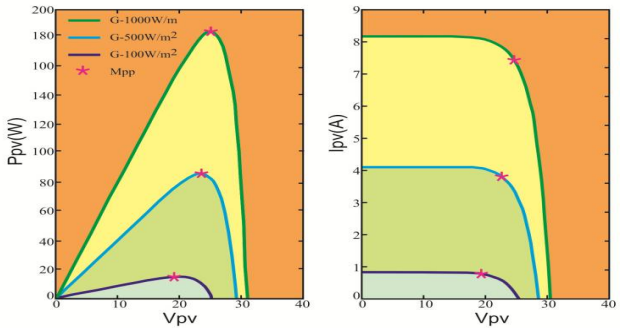

(c)

Preprints (www.preprints.org) | NOT PEER-REVIEWED | Posted: 3 September 2018 doi:10.20944/preprints201809.0031.v1

Peer-reviewed version available at Energies 2019, 12, 167; doi:10.3390/en12010167

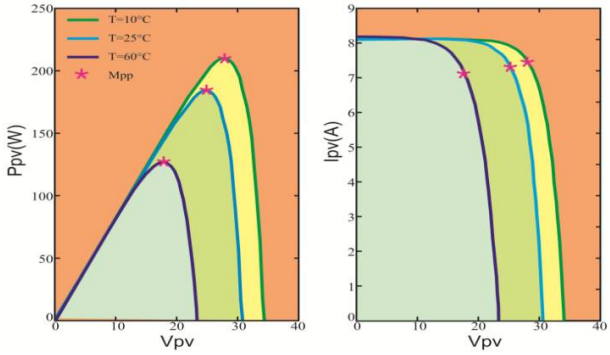

(d)

Figure 1. (a)Standalone hybrid PV-wind- Battery power system (b) Equivalent mode of PV cell (c) and (d) P/V and I/V at different weather profiles (irradiance and temperature.)

2.1. PV Modeling

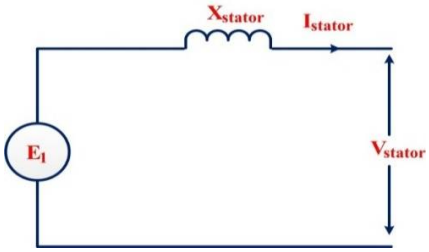

(a)

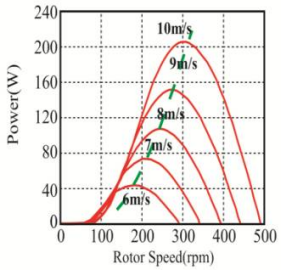

(b)

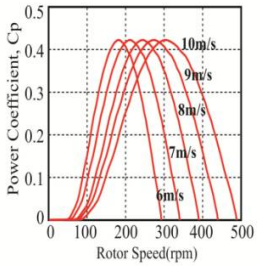

(c)

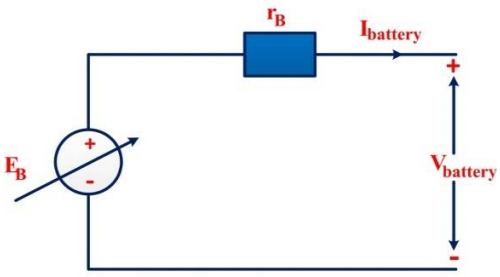

(d)

Figure 2. (a) PMSG model has been developed using steady current (b) Generated power from wind turbine with rotor speed under variable velocity(c) Power factor vs rotor speed with varying wind speed characteristics (d) Electric circuit based battery model.

The equivalent mode of PV cell presented in Fig. 2 (a) comprises current source, diode and series/parallel resistances. The mathematical equations describing output current (I_{out}) based on the electrical circuits can be derived with used abbreviations [22] as:

$$I_{out} = I_{photon} - I_{diode} - I_{PR} \quad (1)$$

Also, I_{photon} can be expressed mathematically as [22]:

$$I_{photon} = \frac{G_A}{G_{REF}}\left[I_{RS\_REF} + P_{SCT}\left(T_C - T_{C\_REF}\right)\right] \quad (2)$$

And

$$I_{diode} = I_{RS}\left[e^{\frac{Q(V_{out}+R_{sr}*I_{out})}{\beta KT}} - 1\right] \quad (3)$$

$$I_{PR} = \frac{1}{R_{PR}}(V_{out} + R_{sr} * I_{out}) \quad (4)$$

$$I_{RS} = \frac{I_{RS\_REF}}{\left[e^{\frac{QV_{open}}{N_S*N*\alpha*T_C}}\right]-1} \quad (5)$$

The output current is equated finally with used abbreviations [22] as:

$$I_{out} = I_{photon} - I_{RS}\left[e^{\frac{Q(V_{out}+R_{sr}*I_{out})}{\beta KT}} - 1\right] - \frac{1}{R_{PR}}(V_{out} + R_{sr} * I_{out}) \quad (6)$$

Non-linear P-V/I-V curves at different weather profiles (irradiance and temperature) are presented clearly in Fig. 2(b) and (c), respectively. For achieving Global Maximum Point (GMP) at every operation, in this work Cukconverter is employed.

2.2. *PMSG Modeling*

To describe the operation of PV-Wind system under intermittent operating conditions, Permanent Magnet Synchronous Generator is employed because of zero reactive power consumption. In addition, it does not have need of gearbox with better power factor and accuracy due to self-execution behavior. The PMSG model has been developed using steady current depicted in Fig. 2 (d). Voltage and current (V_{RE}&I_{RE}) obtained from rectification is expressed [1] mathematically with regard to stator voltage/current (V_{st}, I_{st}).

$$V_{RE} = {3\sqrt{6}}/{\pi}\, V_{stator} \quad (7)$$

$$I_{RE} = {\pi}/{\sqrt{6}}\, I_{stator} \quad (8)$$

2.3. Mathematical Modeling of Wind Turbine System

The produce power rating of wind turbine based on aerodynamic behavior is evaluated mathematically as [1]:

$$P_{Turbine} = {1}/{2} * C_P(\lambda_t, \beta_P)\rho_{air}\pi R_T^2 V_{wind}^3 \quad (9)$$

Where,

$C_P(\lambda_t, \beta_P)$ = Power Coefficient of wind turbine

ρ_{air} = Density of air

R_T = Blade (Wind turbine) radius

V_{wind} = Wind velocity

λ_t = Tip speed ratio

β_P = Pitch blade angle

The turbine tip speed is correlated with wind velocity and wind turbine rotating velocity $\Omega_{Turbine}$ as:

$$\lambda_t = \frac{\Omega_{Turbine} * R_T}{V_{wind}} \tag{10}$$

The power coefficient $C_P(\lambda_t, \beta_P)$ is calculated using mathematical relation as:

$$C_P(\lambda_t, \beta_P) = (0.34 - 0.00166) * (\beta_P - 2) * \sin K * -184 * 10^{-5} (\lambda_t - 3)(\beta_P - 2) \tag{11}$$

And

$$K = \frac{\pi(\lambda_t + 10^{-1})}{1434 * 10^{-2} - 3 * 10^{-1}(\beta_P - 2)} \tag{12}$$

Also,

Mechanical torque $\tau_{mechanical}$ developed using wind turbine is related with produced mechanical power as:

$$\tau_{mechanical} = \frac{P_{mechanical}}{\Omega_{Turbine}} \tag{13}$$

The mechanical relation governing wind turbine system is expressed mathematically as:

$$(J_{Turbine} + J_{Generator}) \frac{d\Omega_{Turbine}}{dt} + f_{viscous} * \Omega_{Turbine} = \tau_{mechanical} - \tau_{EM} \tag{14}$$

$f_{viscous}$= Viscous force

τ_{EM} = Developed electromagnetic torque

Mathematical Modeling of PMSG in dq frame is described as:

$$\begin{bmatrix} \frac{d(I_{sd-axis})}{dt} \\ \frac{d(I_{sq-axis})}{dt} \end{bmatrix} = \begin{bmatrix} \frac{R_{stator}}{L_{d-axis}} & P * \Omega_{Turbine} . L_{q-axis} \\ \frac{P * \Omega_{Turbine} . L_{d-axis}}{L_{q-axis}} & -\frac{R_{stator}}{L_{q-axis}} \end{bmatrix} * \begin{bmatrix} I_{sd-axis} \\ I_{sq-axis} \end{bmatrix} + \begin{bmatrix} V_{sd-axis} \\ \frac{V_{sq-axis} * P\Omega_{Turbine} . \emptyset_{PM}}{L_{q-axis}} \end{bmatrix} \tag{15}$$

Where,

R_{stator} = Stator resistance

L_{d-axis} , . L_{q-axis} = Inductances of Stator winding

$I_{sd-axis}$, $I_{sq-axis}$ = Stator winding current

$\emptyset_{PM}$ = Flux generated by permanent magnet

P = No. of Poles

Fig.3 (a) presents the generated power from wind turbine with rotor speed under variable velocity. Also, the power factor V_s rotor speed with varying wind speed characteristics in Fig. 3(b) demonstrates the optimal power produced from wind turbine achieves at optimal power factor coefficient corresponding.

2.4 Electric Circuit based Battery Model

In this research work, electric circuit based battery model is employed which provides better dynamicity for state of charge approximation. It comprises voltage source (ideal) with series internal resistance, which evaluates battery behavior, depicted using Fig. 3 (c). A Battery (Ni-Cd) discharging characteristic is presented with Fig. 3(d) [22].

Final voltage controlled is obtained mathematically as:

$$V = E_B - \frac{V_{PO} * Q_{Bat}}{Q_{Bat} - \int I_{Battey} dt} + A_{exp}.e(B_{exp} \int I_{Battery}\, dt) \quad (16)$$

Where,

E_B = Battery fixed voltage

V_{PO} = Polarized voltage

Q_{Bat} = Capacity of battery

I_{Battey} = Battery current

A_{exp} = Amplitude of exponential zone

B_{exp} = Inverse time constant exponential zone

2.5. Cuk Converter

The major disadvantages of switched mode power converters have discontinuity of supply current, low dynamic response and higher power device peak current, which made this less acceptable. In contrast with classical switched mode dc-dc converter, Cuk converter comprises less switched power loss, high current behavior with better efficiency, which acts as a power adapter between inverter and renewable sources.

The Cuk converter operation presented in Fig. 4(a) is described in two working modes. When power switch gets short-circuited and energy has been released by capacitor. Table 1 presents the specifications used during design of Cuk converter. The mathematical expression-governing mode-I conducting state is described as:

$$V_{L_A} = V_{in} \quad (17)$$

$$V_{L_B} = -V_{C_A} - V_{C_B} \quad (18)$$

$$I_{C_A} = I_{L_B} \quad (19)$$

$$I_{C_B} = I_{L_B} - \frac{V_{C_B}}{R_{Load}} \quad (20)$$

Preprints (www.preprints.org) | NOT PEER-REVIEWED | Posted: 3 September 2018 doi:10.20944/preprints201809.0031.v1

Peer-reviewed version available at Energies 2019, 12, 167; doi:10.3390/en12010167

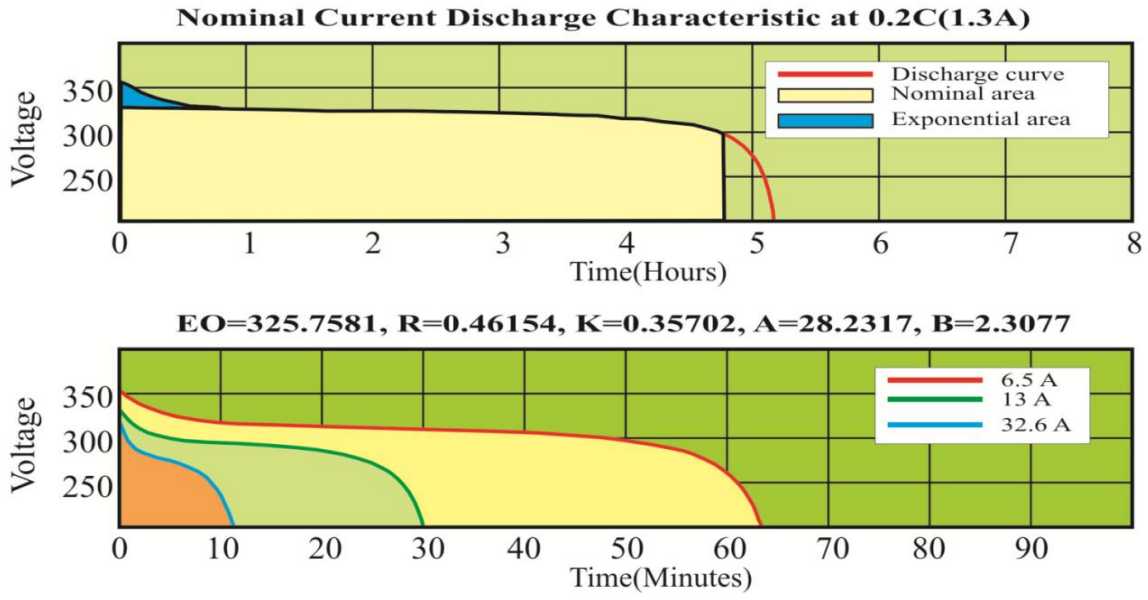

(a)

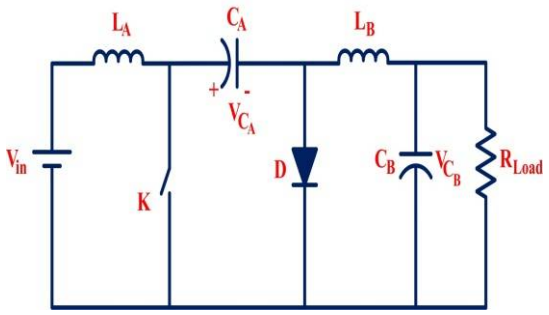

(b)

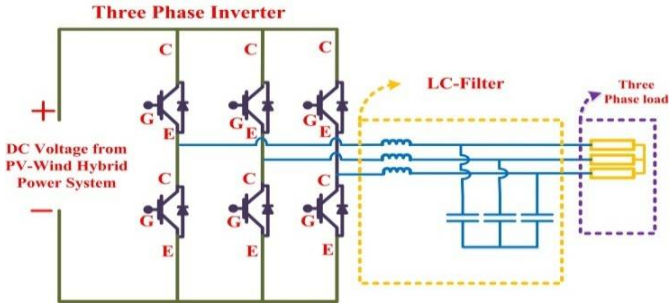

(c)

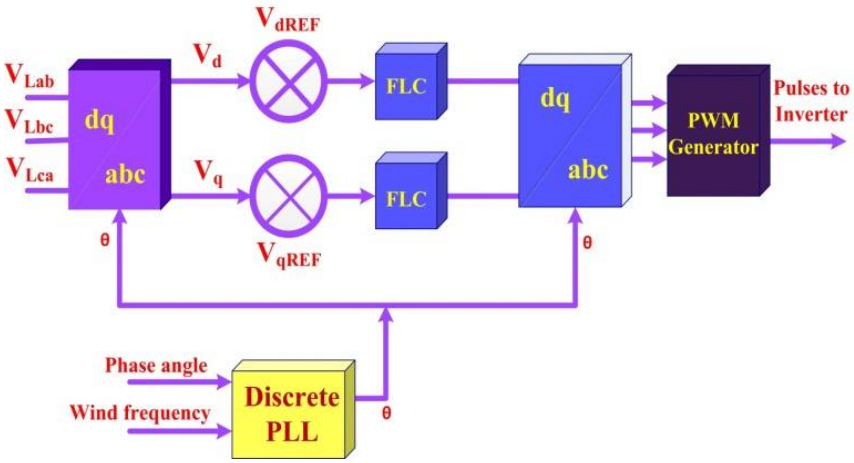

(d)

Figure 3.(a)Battery (Ni-cd) discharging behavior (b)Cuk converter (c) Inverter control (d) FLC regulated inverter controller

Table 1. Cuk converter parameters

S.N.	Parameters	Values
1.	Inductor (L_A=L_B)	0.5 mH
2.	Capacitor (C_A=C_B)	1.5 µF
3.	Frequency of Switching	10 KHz
4.	Diode	500 V/7A
5.	MOSFET (Power Switch K)	600V/12A

In case of power switch gets open circuited, the energy flow takes place with forward biasing diode and input supply is responsible to charge capacitor C_A. Described mathematical relations of this mode of operations are:

$$V_{L_A} = V_{in} - V_{C_A} \quad (21)$$

$$V_{L_B} = -V_{C_B} \quad (22)$$

$$I_{C_A} = I_{L_A} \quad (23)$$

$$I_{C_B} = I_{L_B} - \frac{V_{C_B}}{R_{Load}} \quad (24)$$

3. ANT colony optimization based MPPT

Colorni, Dorigo and Maniezzo invented meta-heuristics based optimized algorithm to solve difficult non-linear issues. The particular ant to obtain the shortest path optimization generates pheromones. For the searching of foods, the movements of ants take place in different direction followed with generated pheromones. The shortest path should have high pheromones probability as it evaporates in short and methodology is repeated for different iterations to optimize the problems.

In this research work, ACO methodology is implemented by considering V_{PV} and I_{PV} followed by generation of target output (V_{Target}). Ants have been situated randomly and its movement is noted to achieve V_{Target} which returns to the colony after this process. Moreover, the V_{Target} and colony distance is treated as duty ratio of Cuk converter. Let A_P variables have targeted to optimize which comprises Y_P produced randomly solutions (Y_P>=A_P). Sampling Gaussian Kernel methodology is used for mathematical description as [16-18]:

$$H_j(y) = \sum_{L=1}^{X} \omega_L h_L^j(y) = \sum_{L=1}^{X} \omega_L \frac{1}{\sigma_L^j * \sqrt{2\pi}} * e^{\frac{-\left(x-\mu_L^j\right)^2}{2\sigma_L^{j^2}}} \quad (25)$$

Where,

$H_j(y)$ = j^{th} Gaussian kernel

$h_L^j(y)$ = j^{th} Gaussian function

σ_L^j = Standard deviation.

μ_L^j = Mean function

Mathematically mean, weight, standard deviations are derived with V_P random solutions.

(I) Mean $(\mu_j) = [\mu_1^j, \ldots, \mu_L^j, \ldots, \mu_x^j]$

(II) Standard deviation $(\sigma_L^j) = \varepsilon_{conv} \sum_{j=1}^{x} \frac{|\mu_i^j - \mu_L^j|}{Y_P - 1}$

(III) Weight $\omega_L = \frac{I}{\sqrt{2\pi} * Q_L * Y_P} e^{\frac{(L-1)^2}{2Q_L^2 K_L^2}}$

ε_{conv} = Rate of convergence

Q_L = Best rank solution

(IV) Probability of Gaussian function selection

$P_L = {\omega_L}/{\sum_{R=1}^{x} \omega_R}$

The proposed sample Process is repeated for optimization of parameters. Let Z_P newly solution are produced and has addition with Y_P initially obtained solution. Total Z_P+Y_P solutions have been obtained in which Y_P best are replicated and overall methodology is recapitulated for several iterations. Table 2 shows ACO parameters used during practical verification. This methodology is stimulated by foraging nature of ants, which are treated as blind living things, and conversion among them takes place-using pheromone alchemical. It comprises positive feedback affection, which provides better-optimized solutions.

Table 2. ACO parameters used during experiment

S.N	Parameters	Values
1.	Total iterations	250
2.	Size of Population	10
3.	Produced random solution	8
4.	Rate of convergence	0.35
5.	Best Rank solution (Q_L)	0.85

4. FLC based inverter control

The inverter depicted in Fig. 4(b) is controlled with Fuzzy logic Control (FLC) based intelligent methodology, which provides the smooth maintenance of load voltage and frequency. Irrespective of wind velocity, loading conditions and level of sun insolation inverter regulates voltage and frequency instant. Fig.4(c) depicts the FLC regulated inverter controller. For maintenance of voltage output (V_{out}) and frequency, a phase locked loop (PLL) presented in Fig 4(c) associated with synchronized frame of reference is employed. The FLC inverter control regulation provides better efficiency, stable operation and less frequency, disturbances with respect to PI based inverter regulation [21]. Fig. 4(d) and 4(e), (f), (g) demonstrate the PWM pulse generation using FLC inverter strategy and membership functions used during implementation.

Preprints (www.preprints.org) | NOT PEER-REVIEWED | Posted: 3 September 2018 doi:10.20944/preprints201809.0031.v1

Peer-reviewed version available at Energies 2019, 12, 167; doi:10.3390/en12010167

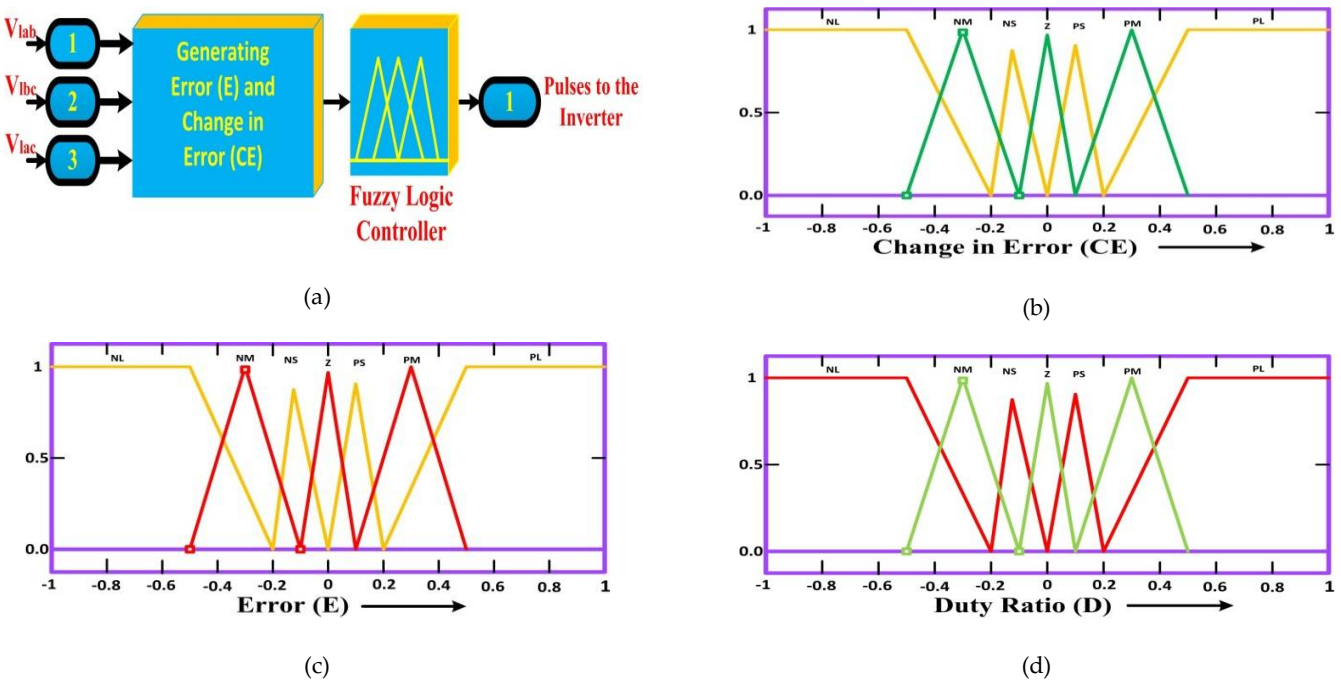

Figure 4. (a)FLC pulse generation (b) Membership functions Error (c) Membership functions change in error (d) Membership functions duty ratio

5. MPPT and inverter controller action with single Cuk converter

CASE me: The two controllers operations are decided based on presence of PV/Wind renewable sources. In case of generation of power from PV as well as wind sources, the ACO based MPPT (controller 1) produces duty ratio for Cuk power converter and FLC inverter control (controller 2) provides power generation from PV and wind renewable sources.

CASE II:In case of power generation from only wind renewable sources (Not PV), the duty ratio of Cuk converter is generated to make DC link voltage fixed and controller 1 works in voltage control mode. In addition to this controller 2 tries to obtain optimal wind power by generating current signal.

CASE III:When PMSG is not in operation and only PV sources are generating power, Cuk converter has no input and there is no pulse generation using controller 1. Controller 2 produces current command signal to obtain optimal PV power generation from PV modules.

6. Experimental set up

Fig. 5(A) depicts the practical set up developed for proposed hybrid (PV-Wind) system controlled through dSPACE, which comprises PV module, wind emulator, Cuk converter, and electric circuit based battery model.

Preprints (www.preprints.org) | NOT PEER-REVIEWED | Posted: 3 September 2018 doi:10.20944/preprints201809.0031.v1

Peer-reviewed version available at Energies 2019, 12, 167; doi:10.3390/en12010167

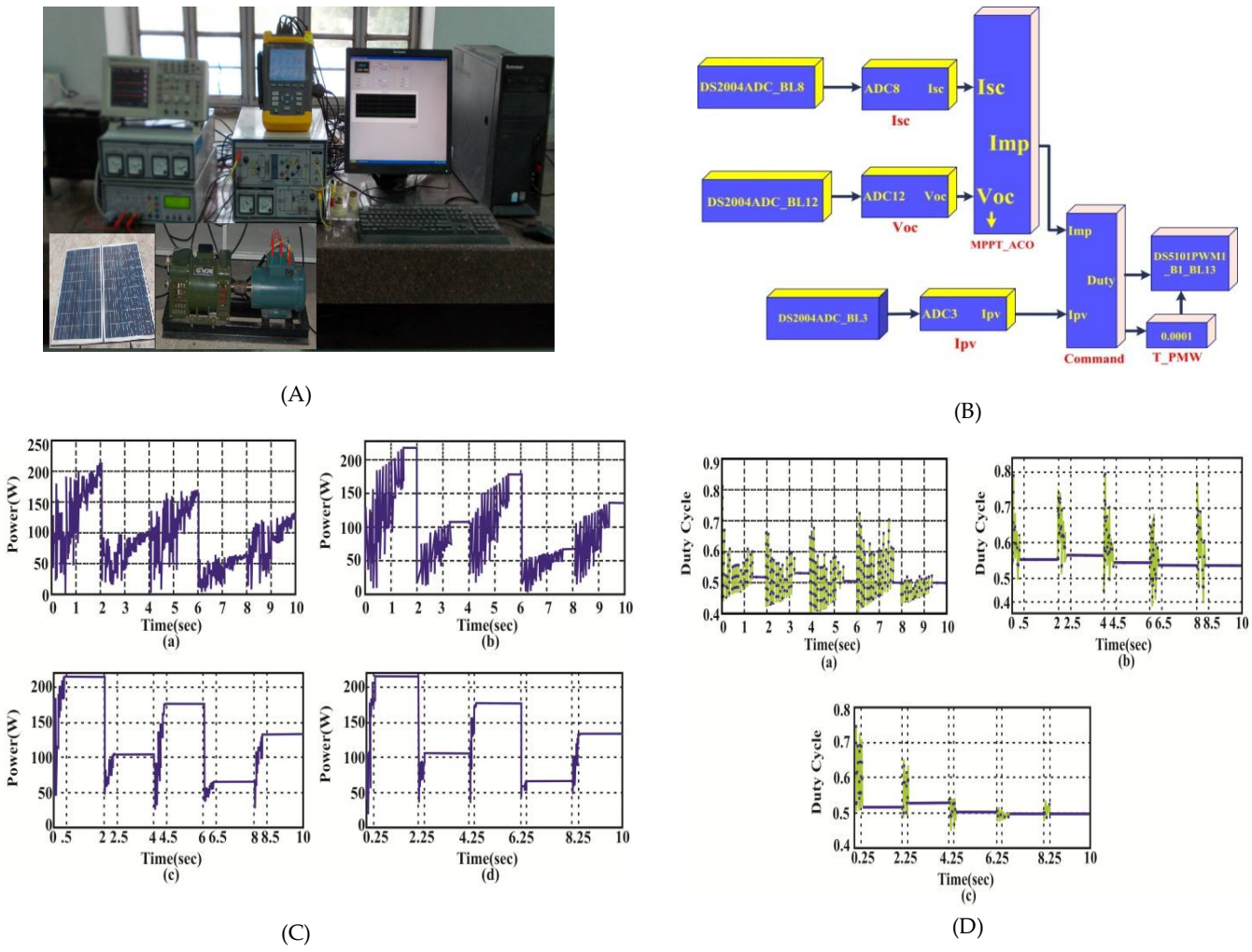

Figure 5. (A)Practical set up developed for proposed hybrid (PV-Wind) system (B) ACO MPPT implementation using dSPACE(C) Power tracking (a) PSO (b) FA(c) ABC (d) ACO (D)Duty ratio (a) PSO (b) ABC (c) ACO

With application of ACO model based MPPT the sensed (Voltage/Current) is transformed to digital pulses by analog to digital converter and controller 1 and controller 2 generated signals are collected from control desk I/O of dSPACE which is processed through insolation interface. LA50- P and LV20-Pcurrent and voltage sensors are employed during experimentation, respectively. The ACO based MPPT is modeled in Fig. 5(B)using MATLAB which generates PWM signal for Cuk converter linked through dSPACE hardware based CT60 AM IGBT, SKHI22 AR gating driver, power supplication using programmed DCMAGNA and PMSG wind emulators are employed during practical investigation.

7. Experimental responses

Practical justification is done by comparing power tracking behavior of ACO algorithm Vs PSO, FA and ABC techniques using Fig.5 (C). The average period required to achieve MPP is presented with comparison using Table 3. The ACO based MPPT method takes lesser time compared to other algorithms mentioned. Moreover, the duty ratio performance with ACO MPPT is better compared to other techniques employed in Fig. 5 (D).Fig. 6 (A) portrays the starting operation before GMP achievements in which PV module voltage level tries to reach preset level of voltage.

Preprints (www.preprints.org) | NOT PEER-REVIEWED | Posted: 3 September 2018 doi:10.20944/preprints201809.0031.v1

Peer-reviewed version available at Energies 2019, 12, 167; doi:10.3390/en12010167

The steady state behavior of the designed PV system is also examined and is justified with matched PV characteristics depicted by Fig. 6(B). By means of proposed intelligent ACO, the inverter current becomes synchronized and in phase with grid utility voltage depicted by responses in Fig. 6(C). The dynamic performance of ACO based PV power system has been justified with variations in fluctuating sun insolation and can be depicted in Fig. 6(D). Fig. 7(a) demonstrates the responses obtained from hybrid PV-wind controlled ACO, which clearly interprets that MPPT operation is achieved independently without influencing one another.

Table 3. Performance MPPT comparison

S.N	Techniques	Tracking Time (Avg)
1.	PSO	5.1 s
2.	FA	2.75 s
3.	ABC	0.75 s
4.	ACO	0.38 s

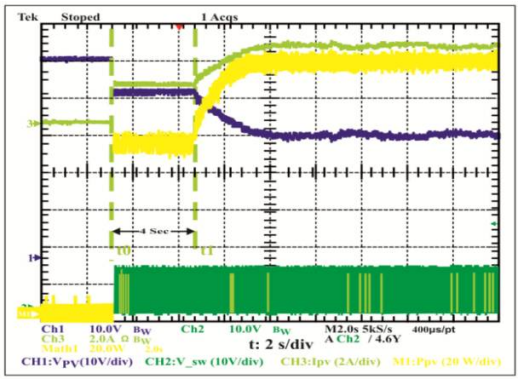

(a)

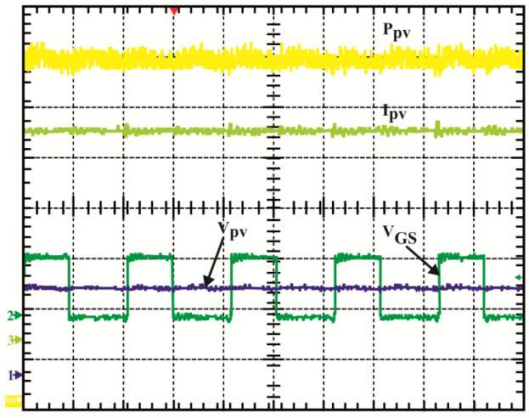

(B)

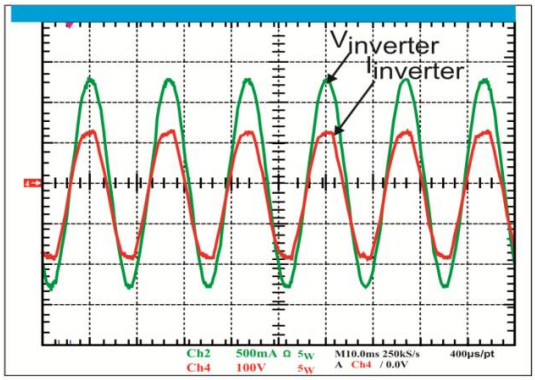

(a)

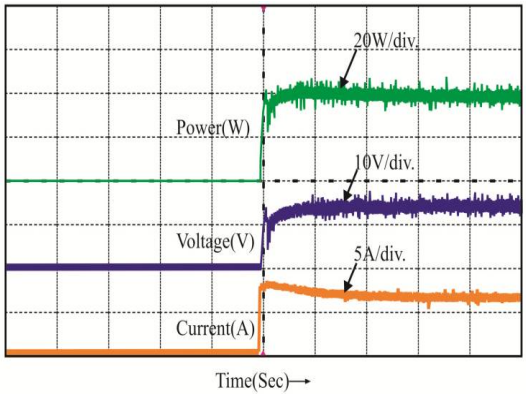

(b)

Figure 6. (A) Starting operation PV MPPT (B) Steady state behavior of the designed PV system (C) Inverter current becomes synchronized and in phase with grid, utility voltage (D) ACO based PV power system with variations in fluctuating sun insolation

The intermittent behavior of PV-wind system with proposed methodology is accurately tested experimentally using proposed algorithm. Abruptly, the PV-wind power system has been turned ON/OFF and

Preprints (www.preprints.org) | NOT PEER-REVIEWED | Posted: 3 September 2018 doi:10.20944/preprints201809.0031.v1

Peer-reviewed version available at Energies 2019, 12, 167; doi:10.3390/en12010167

output responses are noted under these operating situations. Fig. 7(b) presents the responses of hybrid system when wind turbine gets turns ON/OFF abruptly. It is clearly visualized that the PV system works independently and provides output power without influencing one another. The PV/Wind renewable sources are transferring power one of two concurrently or particularly. Complementary, the performance of hybrid PV-Wind system is evaluated when PV system is turned ON/OFF which does not influence the wind turbine operation when abrupt changes occurs in PV system, which is depicted in Fig. 7(c). The transient performance of the hybrid control system has been evaluated by keeping wind condition constant and sun insolation variable. The corresponding change in V_{PV}, I_{PV} and $I_{battery}$ is noted under fluctuating sun irradiance. Battery gets charge and discharge depending on increasing/decreasing nature of solar insolation, which maintains the terminal voltage fixed and validates the effective design of proposed algorithms regulation.The power output generations from hybrid (PV and Wind) energy sources are compared using Fig. 8 (a) and (b), respectively using PI and FLC regulated inverter control. In case of PI based inverter controller, voltage output (V_{out}) is found unstable and has more frequency perturbation in contrast to FLC based inverter control illustrated using Fig. 8 responses.

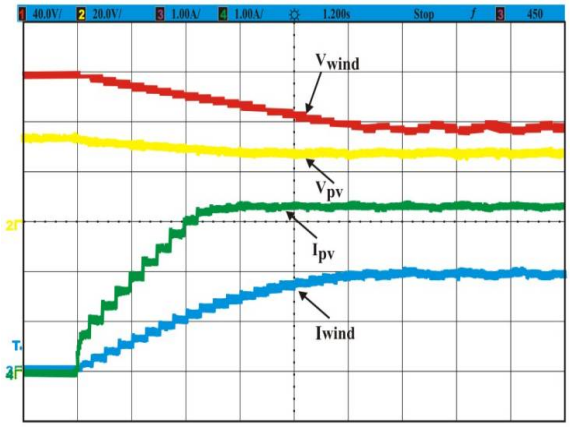

(a)

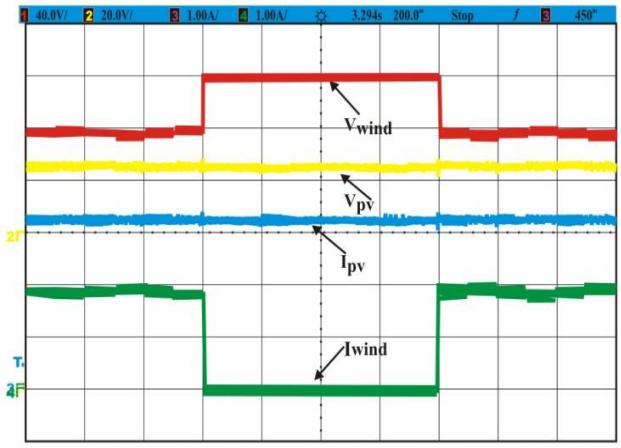

(b)

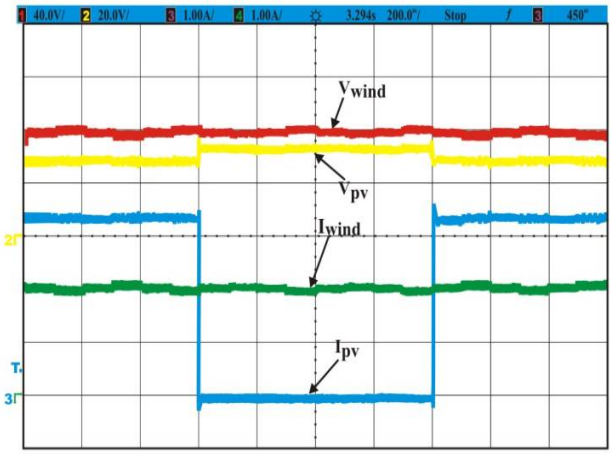

(c)

Figure 7. (a) PV-wind MPPT operation without influencing one another (b) Responses of hybrid system when wind turbine gets turns ON/OFF abruptly (c) Performance of hybrid PV-Wind system is evaluated when PV system gets turned ON/

Preprints (www.preprints.org) | NOT PEER-REVIEWED | Posted: 3 September 2018 doi:10.20944/preprints201809.0031.v1

Peer-reviewed version available at Energies 2019, 12, 167; doi:10.3390/en12010167

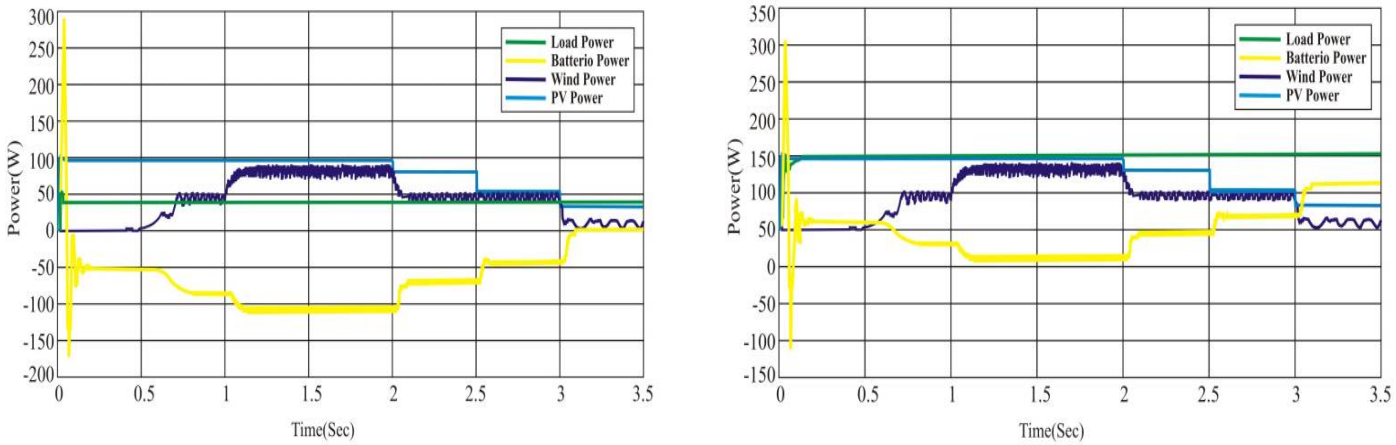

Figure 8. Transient performance of the hybrid control system (a) FLC inverter control (b) PI-control

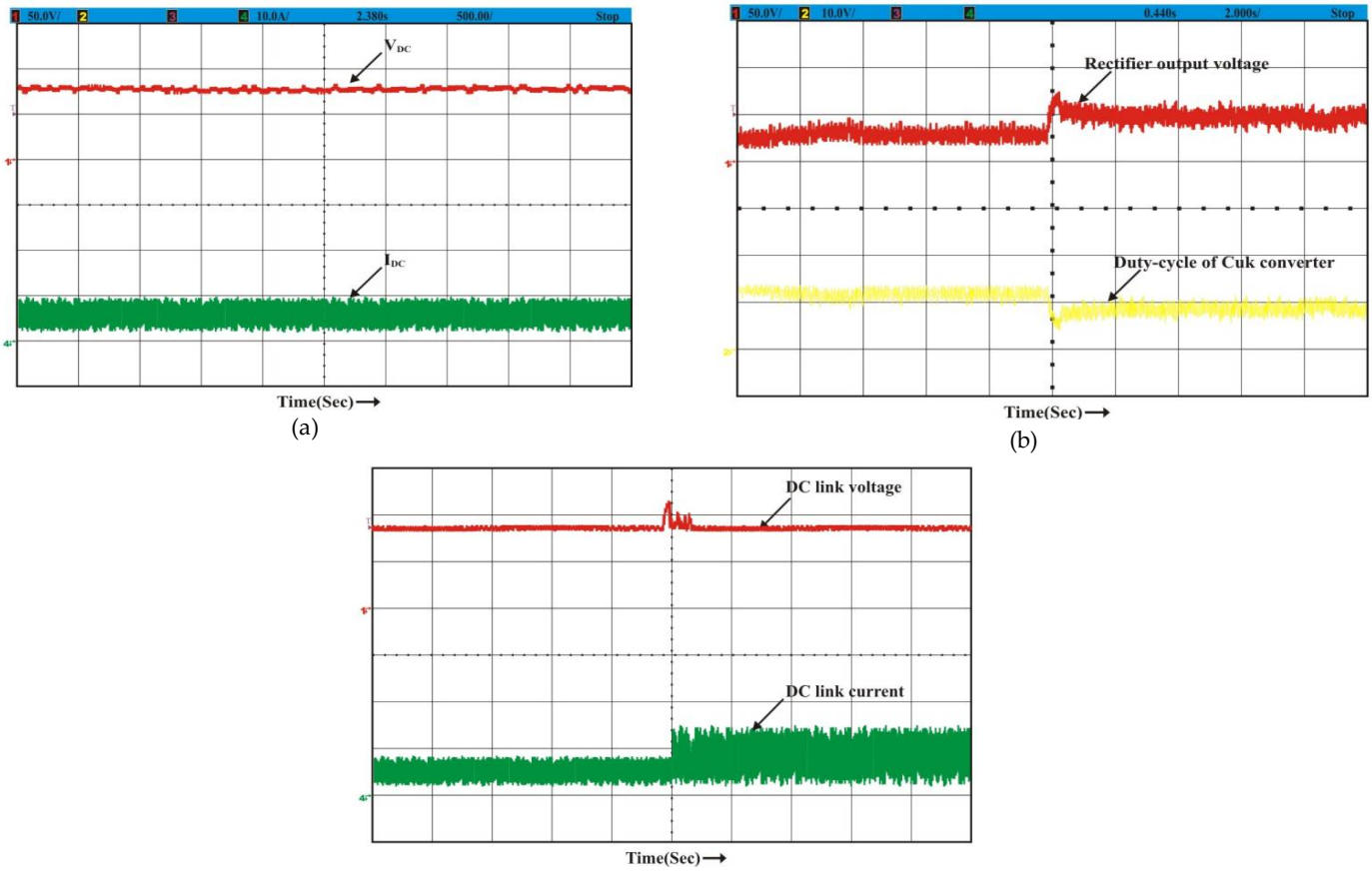

Figure 9. (a)Steady state operating conditions, the DC link voltage/current (b) Dynamic behavior of proposed hybrid power system variation in $V_{Rectifier}$ and Cuk converter duty ratio **(c).** Corresponding rectifier waveforms and DC link voltage/current

Under steady state operating conditions, the DC link voltage/current is noted under variable solar insolation 400 W/m^2 and PMSG turbine velocity 5*10^{-1}p.u. is illustrated using Fig. 9(a). The dynamic behavior of proposed hybrid power system is tested under operating conditions (Fixed Sun insolation 700 W/m^2 and increment in PMSG

shaft velocity 0.5 to 0.75 p.u). Therefore, consequent variation in $V_{Rectifier}$ and Cuk converter duty ratio is reported to keep DC link voltage fixed explained using Fig. 9(b). Fig.9(c) illustrates the corresponding rectifier waveforms and DC link voltage/current obtained during experimentation. The reliable operation of PV-Wind system with ACO MPPT control has been practically substantiated using dSPACE interface. Table 4 demonstrates the used PV and Wind turbine specifications for practical justification.

8. Conclusion

Under extreme varying environmental conditions, the ACO based optimized methodology provides optimal power extraction from solar and wind energy sources for residential applications, which contained high convergence velocity, better-searched performance and simpler implementation as major advantage. The completed hybrid solar wind driven PMSG power system is modeled through MATLAB and provides hardware interface (dSPACE) for validation and confirmation of high power generation. Under low wind velocity, the hybrid system has low battery consumption, which demonstrates the improved controller performance. Inverter regulated with FLC-dSPACE control has power efficiency equated with classical PI-controller. The hybrid integration of solar and wind energy system have been realized experimentally under various conditions to develop novel hybrid power system followed by Cukconverter.ACO algorithms developed using m-file has complex coding interfaced to dSPACE hardware board. Included work can be extended to learning framework with internet of things based intelligent algorithms for PV-Wind hybrid system to achieve utmost power tracking efficiency.

Table 4. PV and Wind turbine specifications

S.N	Parameters	Values
1.	PV rated power	200W
2.	Wind generation (Rated)	200W
3.	Stator and Rotor resistance	4.3Ω , 3.8Ω
4.	No. of Poles	4

References

1. Singaravel, M.M.R.; Daniel, S.A.MPPT with Single DC-DC Converter and Inverter for Grid Connected Hybrid Wind-Driven PMSG-PV System.*IEEE Trans. on Ind. Electron*. **2015**, 62, 4849-4857.
2. Chen, -YM.; Liu, -YC.; Hung, –SC.; Cheng, –CS.Multi-Input Inverter for Grid-Connected Hybrid PV/Wind Power System.*IEEE Trans. on Ind. Electron*.**2007**, 22, 1070-1077.
3. Wandhare, R.G.;Agarwal, V.Novel Integration of PV-Wind Energy System with Enhanced Efficiency. *IEEE Trans. on Power Electron*.**2015**, 30, 3638-3649.
4. Geng, H.; Liu, L.; Li, R.Synchronization and Reactive Current Support of PMSG based Wind Farm during Severe Grid Fault. *IEEE Trans. on Sustainable Energy*. **2018**, 1-1.
5. Das, S.;Subudhi, B.A *Hinfty* Robust Active and Reactive Power Control Scheme for a PMSG based Wind Energy Conversion System. *IEEE Trans. on Energy Conversion*.**2018**, 1-8.
6. Ahmed, J.; Salam, Z. An Enhanced Adaptive P&O MPPT for Fast and Efficient Tracking Under Varying Environmental Conditions. *IEEE Trans. on Sustainable Energy*. **2018**, 9, 1487-1496.
7. Xiao, X.; Huang, X.; Kang, Q. A Hill Climbing Method-Based Maximum Power Point-Tracking Strategy for Direct-Drive Wave Energy Converters.*IEEE Trans. on Ind. Electron*. **2016**, 63, 257-267.
8. Kumar, N.; Hussain, I.; Singh, B.; Panigrahi, B.K. Self-Adaptive Incremental Conductance Algorithm for Swift and Ripple Free Maximum Power Harvesting from PV Array. *IEEE Trans. on Ind. Info*.**2018**, 14, 2031-2041.

9. Khateb, A.E1.; Rahim, N.A.; Selvaraj, J.;Uddin, M.N.Fuzzy Logic Controller Based SEPIC Converter for Maximum Power Point Tracking.*IEEE Trans. on Ind. Appl.*, **2014**, 50, 2349-2358.
10. Lin, -WM.; Hong, –CM.; Chen, –CH.Neural-Network-Based MPPT Control of a Stand-Alone Hybrid Power Generation System.*IEEE Trans. on Power Electron*. **2011**, 26, 3571-3581.
11. Koad, R.B.A.;Zobaand, A.F.;Shahat, A.E1. A Novel MPPT Algorithm Based on Particle Swarm Optimisation for Photovoltaic Systems.*IEEE Trans. on Sustainable Energy*.**2017**, 8, 468-476.
12. Sundareswaran, K.; Peddapati, S.; Palani S. MPPT of PV Systems under Partial Shaded Conditions through a Colony of Flashing Fireflies.*IEEE Trans. on Energy* Conversion.**2014**, 29, 463-472.
13. Sundareswaran, K.; Sankar, P.; Nayak, P.S.R.; Simon, S.P.; Palani, S. Enhanced Energy Output From a PV System Under Partial Shaded Conditions Through Artificial Bee Colony.*IEEE Trans. on Sustainable Energy*.**2015**, 6**,** 198-209.
14. Ram, J.P.; Rajasekar, N. A novel Flower Pollination based Global Maximum Power Point method for Solar Maximum Power Point Tracking. *IEEE Trans. on Power Electron*.**2017**, 32, 8486-8499.
15. Mohanty, S.; Subudhi, B.; Ray, P.K.A Grey Wolf Assisted Perturb & Observe MPPT Algorithm for a PV System. *IEEE Trans. on Energy Conversion*.**2017**, 32, 340-347.
16. Belhachat, F.; Larbes, C. Global maximum power point tracking based on ANFIS approach for PV array configurations under partial shading conditions. *Elsevier Renewable and Sustainable Energy Reviews*.**2017**, 77, 875–889.
17. Sundareswaran, K.; Kumar, V.V.; Sankar, P.; Simon S,P.; Nayak, P.S.R.; Palani, S. Development of an improved P&O algorithm assisted through a colony of foraging ants for MPPT in PV system. *IEEE Trans. on Ind. Info.***2016**, 12, 187-200.
18. Emerson, N.;Srinivasan, S. Integrating Hybrid Power Source into Islanded Micro grid Using Ant Colony Optimization. In Proc. of Int. Conf. on Advanced Computing and Communication Systems (ICACCS -2015). **2015**, pp. 1-4.
19. Banaei, M.R.; Sani, S.G. Analysis and implementation of a new SEPIC-based single switch buck-boost dc-dc converter with continuous input current. *IEEE Trans. on Power Electron*.**2018**, 1-1.
20. Deepak.;Pachauri, R.K.;Chauhan, Y. K.Modeling and Simulation Analysis of PV Fed Cuk, Sepie, Zeta and Luo DC-DC Converter. In Proc. of Int. Conf. on Power Electron. Intelligent Control and Energy Systems (ICPEICES-2016).**2016**, pp. 1-6.
21. Farhat, M.; Barambones, O.; Sbita, L.Efficiency boosting for PV systems using new MPPT method. In Proc. of 23rdMediterranean Conf. on Control and Automation (MED). **2015**, pp. 777-782.
22. Saidi, A.;Chellali, B.Simulation and Control of Solar Wind Hybrid Renewable Power System. In Proc. of 6thInt. Conf. on Systems and Control. **2017**, pp. 51-56.